

Magnetohydrodynamic mixed convection in a nanofluid filled tubular enclosure

Abstract

Mixed convection flow in a tubular enclosure filled with nanofluid in the presence of a magnetic field is numerically investigated in the present study. The bottom and top curved wall of the enclosure are respectively kept isothermally hot and cool while the remaining walls are insulated. The governing equations are formulated based on Boussinesq assumptions and solved with finite element method. The computation is carried out for mixed convection regime ($0.1 \leq Ri \leq 10$) and also natural convection regime ($10 < Ri \leq 100$) with fixed values of remaining parameters. A detailed parametric discussion is presented for the physical properties of flow and temperature distributions in terms of streamlines, isotherms, average heat transfer rate within the flow domain. The results show that the flow and temperature fields affected by varying of pertinent parameters. Moreover, heat transfer rate is increased by 139.50% with the increase in Richardson number from 0.1 to 100. The increasing rate of heat transfer due to Ri is respectively decreased by 58.11% with varying of Ha from 0 to 60 and increased by 23.97% with the addition of nanoparticles up to 3%. Comparison is performed against the previously published results on the basis of special cases and found to be in excellent agreement.

Keywords: magnetic field, mixed convection, nanofluids, finite element method, tubular enclosure

Volume 4 Issue 1 - 2020

Rowsanara Akhter,¹ MA Alim,² M A Maleque,² MM Ali³

¹Department of Electrical and Electronic Engineering, International University of Scholars, Bangladesh

²Department of Mathematics, Bangladesh University of Engineering and Technology, Bangladesh

³Department of Mathematics, Mawlana Bhashani Science and Technology University, Bangladesh

Correspondence: Mohammad Mokaddes Ali, Department of Mathematics, Mawlana Bhashani Science and Technology University, Tangail-1902, Bangladesh, Email mmal309@gmail.com

Received: February 03, 2020 | **Published:** March 19, 2020

Introduction

Combined convections free and forced, named as mixed convection in closed enclosure is essential in thermal engineering due to its frequent occurrences in heat transfer processes. In addition, the application of magnetic field effect on mixed convection within closed enclosure received a substantial attention by the researchers and engineers. Several investigators accomplished theoretical and experimental works on mixed convection within different geometries. Rahman et al.¹ investigated mixed convection in a rectangular cavity in presence of an internal heat conducting cylinder with different orientations. They found that heat conducting cylinder of different sizes and locations strongly affects the flow and temperature distributions within the cavity. They also noted that heat transfer rate becomes highest while cavity aspect ratio is 0.5 compared to the other cases. Later on, Basak et al.² studied the mixed convection in a lid driven porous cavity with different thermal conditions by using penalty finite element analysis. Their results indicated that the enhancement of local and average Nusselt number depends on the relevant physical parameters as well as thermal conditions. USR finite difference method was utilized by Ismael et al.³ to analyze mixed convection in a square cavity with two moving horizontal walls. They also introduced partial slip mechanism to the moving walls. The convection declined with partial slip parameter. Moreover, average Nusselt number became higher with Richardson number at nonzero slip parameter. After that, Mittal et al.⁴ extended this analysis³ for a porous cavity with two vertical moving walls filled with nanofluids. Their results indicated that heat transfer rate increases significantly due to the presence of nanoparticles. It was also noted that average Nusselt number is an increasing function of solid volume fraction. Ali et al.^{5,6} performed numerical studies of mixed convection in different geometries in presence magnetic field effects. They suggested that heat transfer rate depends on the variation of physical parameters along with geometrical configurations. In addition, heat transfer rate decreased with the increase in magnetic field strength. Rashidi et al.

exercised mixture model to investigate mixed convection in a vertical wavy channel filled with nanofluids. They found that heat transfer rate increases with increasing of Grashof number and Reynolds number for nanofluids with different concentration of nanoparticles. Later on, finite volume method was implemented by Kareem et al.⁸ to simulate mixed convection in a lid-driven trapezoidal cavity filled with nanofluids and they showed the heat transfer rate increases for increasing concentration of nanoparticles. The increasing rate of heat transfer due to volume fraction diminished with the diameter of nanoparticles. After that, Javed et al.⁹ conducted a similar study⁸ under the effects of uniformly and non-uniformly heating conditions in presence of magnetic field. They observed convection is dominant at higher Rayleigh number and local Nusselt number is maximum at the edges and minimum at centre of the cavity. From the open literature review, it is clear that no study has been conducted for mixed convection in tubular enclosure. In respect of technological view, heat transfer and fluid motion in tubular enclosure have a significant role in thermal engineering. The specific of objectives of this study were to analyze the fluid flow and temperature distribution for magnetohydrodynamic mixed convection in tubular enclosure filled with nanofluid. The numerical solutions have been carried out using finite element method, and for a range of Richardson number, Hartman number and volume fraction with fixed values of other physical parameters. The results have been presented in terms of streamlines and isotherms. The values of average Nusselt number at the heated surface to the fluid domain are also presented graphically. The numerical results of the current study has been compared with the previous studies to show the validity of the present simulation. The present study has been arranged in the following way: Section 2 illustrates physical model of the current study; Section 3 contains mathematical analysis, computational procedure, grid refinement test, validation of numerical procedure; Results based on the numerical simulation have been discussed in detailed in section 4. Finally, conclusion has been drawn in section 5.

Nomenclature:

c_p	Specific heat at constant pressure	$(kJ\ kg^{-1}\ K^{-1})$
g	Gravitational acceleration	$(m\ s^{-2})$
Gr	Grashof number	$g\beta_f(T_h - T_c)L^3 / \nu_f^2$
Ha	Hartmann number	$B_0 L \sqrt{\sigma_f / \mu_f}$
L	Length of the enclosure	(m)
h	Local heat transfer coefficient	$(W\ m^{-2}\ K^{-1})$
k	Thermal conductivity	$(W\ m^{-1}\ K^{-1})$
Nu	Nusselt number	$Nu = hL / k_f$
Pr	Prandtl number	$Pr = \nu_f / \alpha_f$
p	Dimensional pressure	$(N\ m^{-2})$
P	Dimensionless pressure	
q_w	Heat flux	$(W\ m^{-2})$
Re	Reynolds number	$u_i L / \nu_f$
Ri	Richardson number	Gr / Re^2
T	Dimensional temperature	(K)
u, v	Dimensional velocity components	$(m\ s^{-1})$
U, V	Dimensionless velocity components	
x, y	Dimensional coordinates	(m)
X, Y	Dimensionless coordinates	
Greek symbols		
α	Fluid thermal diffusivity	$(m^2\ s^{-1})$
β	Thermal expansion coefficient	(K^{-1})
ϕ	Volume fraction of nanoparticles	
θ	Dimensionless temperature	$\theta = (T - T_c) / (T_h - T_c)$
μ	Dynamic viscosity	$(N\ s\ m^{-2})$
ν	Kinematic viscosity	$(m^2\ s^{-1})$
ρ	density	$(kg\ m^{-3})$
Subscripts		
f	fluid	
h	hot	
c	cold	
nf	nanofluid	

Physical model

The physical model of the problem is presented in Figure 1. The bottom curved wall of the enclosure is heated with isothermal temperature T_h and the top curved wall is cooled with temperature T_c ($T_h > T_c$) while the horizontal walls are maintained adiabatic condition. The x -axis is considered along the horizontal direction and y -axis is normal to it. Gravitational force is acted in the vertically downward direction. Uniform magnetic field of strength B_0 is imposed along the horizontal direction. The working fluid within the enclosure is water based nanofluid containing CuO nanoparticles. The thermophysical properties of the base fluid and CuO nanoparticles have been given in Table 1.

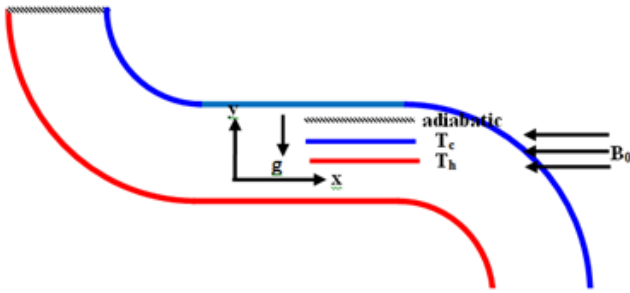


Figure 1 Schematic diagram of the physical system.

Table 1 Thermo physical properties of base fluid and copper-oxide¹⁰

Physical properties	Base fluid	Copper-oxide (CuO)
C_p (J / kgK)	4179	540
ρ (kg / m ³)	997.1	6500
k (W / mK)	0.613	18
β (1 / K)	2.1×10^{-4}	0.085×10^{-4}
σ ($\Omega.m$) ⁻¹	0.05	10^{-10}

Mathematical analysis

Using the Boussinesq approximation the mathematical model can be written as follows 1,2,5,6,8:

$$\frac{\partial U}{\partial X} + \frac{\partial V}{\partial Y} = 0 \quad (1)$$

$$U \frac{\partial U}{\partial X} + V \frac{\partial U}{\partial Y} = -\frac{\partial P}{\partial X} + \frac{\nu_{nf}}{Re} \left(\frac{\partial^2 U}{\partial X^2} + \frac{\partial^2 U}{\partial Y^2} \right) \quad (2)$$

$$U \frac{\partial V}{\partial X} + V \frac{\partial V}{\partial Y} = -\frac{\partial P}{\partial Y} + \frac{\nu_{nf}}{Re} \left(\frac{\partial^2 V}{\partial X^2} + \frac{\partial^2 V}{\partial Y^2} \right) + \left(\frac{\beta_{nf}}{\beta_f} \right) Ri \theta - \left(\frac{\rho_f}{\rho_{nf}} \right) \left(\frac{\sigma_{nf}}{\sigma_f} \right) \frac{Ha^2}{Re} V \quad (3)$$

$$U \frac{\partial \theta}{\partial X} + V \frac{\partial \theta}{\partial Y} = \frac{\alpha_{nf}}{\alpha_f Pr Re} \left(\frac{\partial^2 \theta}{\partial X^2} + \frac{\partial^2 \theta}{\partial Y^2} \right) \quad (4)$$

The above equations have been non-dimensionalized using the following dimensionless quantities 2:

$$X = \frac{x}{L}, Y = \frac{y}{L}, U = \frac{u}{U_0}, V = \frac{v}{U_0}, P = \frac{p}{\rho_{nf} U_0^2} \text{ and } \theta = \frac{T - T_c}{T_h - T_c} \quad (5)$$

The physical parameters of the governing equations (1-4) are Reynolds number (Re), Hartmann number (Ha), Prandtl number (Pr) and Richardson number (Ri), which are defined as:

$$Re = \frac{U_0 L}{\nu}, Ha = \sqrt{\frac{\sigma B_0^2 L^2}{\mu}}, Pr = \frac{\nu_f}{\alpha_f} \text{ and } Ri = \frac{Gr}{Re^2}$$

and the appropriate boundary conditions for the present problem are given below :

$$\text{At the top curved surface: } U=V=0, \theta=0. \quad (6)$$

$$\text{At the top horizontal surface: } U=V=0, \frac{\partial \theta}{\partial Y}=0. \quad (7)$$

$$\text{At the bottom horizontal surface: } U=1, V=0, \frac{\partial \theta}{\partial Y}=0. \quad (8)$$

$$\text{At the bottom curved surface: } U=V=0, \theta=1. \quad (9)$$

The heat transfer rate is calculated in terms of local Nusselt number along the heated section of the enclosure which is defined in dimensionless form as:¹⁰

$$\bar{Nu} = -\frac{k_{nf}}{k_f} \frac{\partial \theta}{\partial X} \quad (10)$$

And the average Nusselt number is calculated by integrating the local Nusselt number along the heated curved surface which is given by¹¹

$$Nu = (1/L) \int_0^L \bar{Nu} dY \quad (11)$$

Computational procedure

Galerkin weighted finite element method has been implemented to simulate the governing equations which have been described in detailed by Taylor & Hood¹² and Dechaumphai¹³ where the computational domain has been discretized into finite elements by using non-uniform triangular elements.

Grid refinement test

To obtain an appropriate grid size for the present simulation, a grid independent test has been performed for average Nusselt number using five types of meshes at certain values of controlling parameters. The values of average Nusselt number in Table 2 and Figure 2 reflects that average Nusselt number at the grid size of 5721 nodes and 10922 elements has a little difference with the next grid size. Accordingly, it can be concluded that further refinement of meshing will have no significant impact on the results. Thus, the grid size of 5721 nodes and 10922 elements provides a satisfactory solution for the present analysis.

Validation of numerical procedure

The numerical procedure of the present study has been validated against the identical problem of Basak et al.¹⁴ and Rahman & Alim.¹⁵ Comparisons of the present results with the results of the aforesaid investigators^{14,15} have been presented in Figure 3 & Table 3, respectively. Figure 3 shows the comparison between stream function

and temperature contours^{14,15} with the present simulation and Table 3 represents the comparative results of average Nusselt number for varying of Hartmann number. Comparing the graphical and numerical results in Figure 3 and Table 3, a reasonable agreement has been obtained between the present results and the aforesaid results.

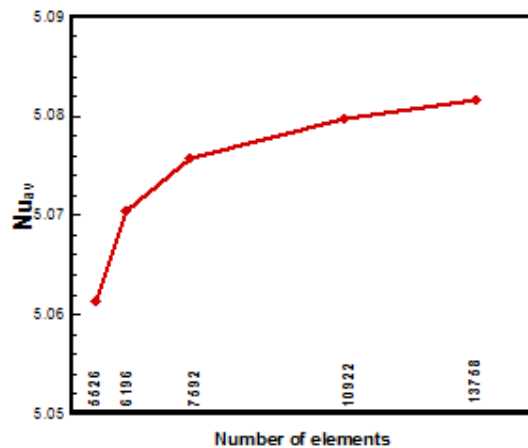


Figure 2 Grid refinement test.

Table 2 Grid sensitivity test at $Pr = 6.2$, $Ri = 1.0$, $Ha = 10$ and $Re = 50$

Nodes (elements)	2852 (5526)	3254 (6196)	3294 (7592)	5721 (10922)	7189 (13758)
Nu_{av}	5.06138	5.07044	5.07582	5.07969	5.08156

Table 3 Comparison of average nusselt number (Nu_{av}) for various hartmann number

Ha	Rahman and Alim ¹⁵	Present study	Error (%)
0	2.2	2.17	1.3
10	2.11	2.11	0
20	1.82	1.84	1.1
50	1.18	1.21	2.5

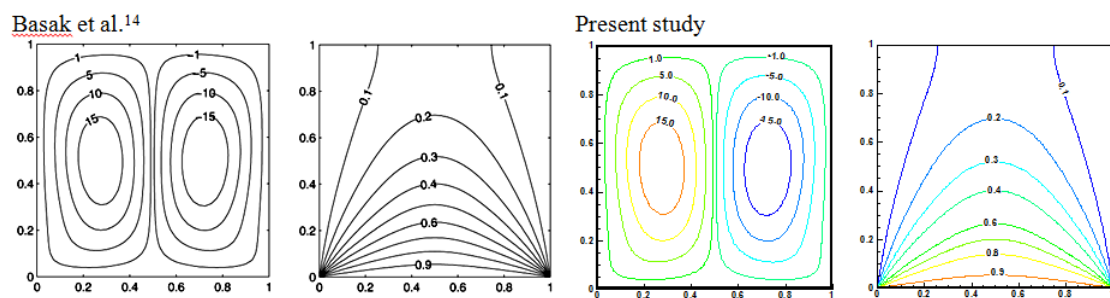


Figure 3 Comparison of stream function and temperature contours.

Results and discussion

The numerical results of flow and temperature fields for magnetohydrodynamic mixed convection flow in a tubular enclosure filled with water based nanofluid have been plotted in this section and then illustrated in terms of streamlines and isotherms and also heat transfer rate through average Nusselt number, respectively. Figure 4 illustrates streamlines and isotherms for the effects of Richardson number while $Pr = 6.2$, $Ha = 10$, $\phi = 1\%$ and $Re = 50$. The different values of Richardson number represent three convection dominant phenomena (e. g. forced convection dominant with $Ri < 1$, mixed convection for $Ri = 1$ and free convection for $Ri > 1$). From Figure 4(a), it is seen at $Ri = 0.1$, two complete circulations and one incomplete circulation are developed within the enclosure where the complete circulations are rotated in clockwise direction and incomplete is in counter clockwise rotation. It is also observed that the pattern of flow circulation is slightly changed with higher strength while Ri increases up to 1. Moreover, the trend of flow pattern changes rapidly from mixed convection regime to free convection dominant regime for varying of Ri (> 1) and the number of complete vortices increases with greater strength for increasing of Ri which indicates the free convection dominant regime for $Ri \geq 10$ that cases greater heat

transfer rate. The physical fact behind is that the mechanical effect of greater Ri increases the buoyancy force to influence the flow field. On the other hand, in Figure 4(b), it is seen that the isotherm contours are similarly distributed within the forced and mixed convection regimes. Moreover, isotherm contours bended with increasing Ri and condensed towards the hot and cold surfaces. In addition, temperature plotting changes noticeably with higher Ri . Thus, significant changes are observed in the convection dominant region than in mixed convection region because the buoyancy force due to greater Ri becomes more predominant. Figure 5 demonstrates the variation of heat transfer rate for varying in Ri in terms of average Nusselt number with four different values of Ha and ϕ . From these figures, it is seen that heat transfer rate increases monotonically with the increase in Ri for each of Ha and ϕ , respectively. Moreover, the increasing rate of heat transfer respectively declines and accelerates with higher magnetic effect as well as concentration of nanoparticles. The physical fact behinds it's that magnetic field effect increases the fluid temperature which reduces the temperature differences between the hot surface and fluid domain. Besides this, addition of nanoparticles in to the base fluid increases the heat transfer capability. Moreover, heat transfer is insignificant in forced and mixed convection regime ($Ri \leq 1$) compared to free convection regime ($Ri \geq 1$).

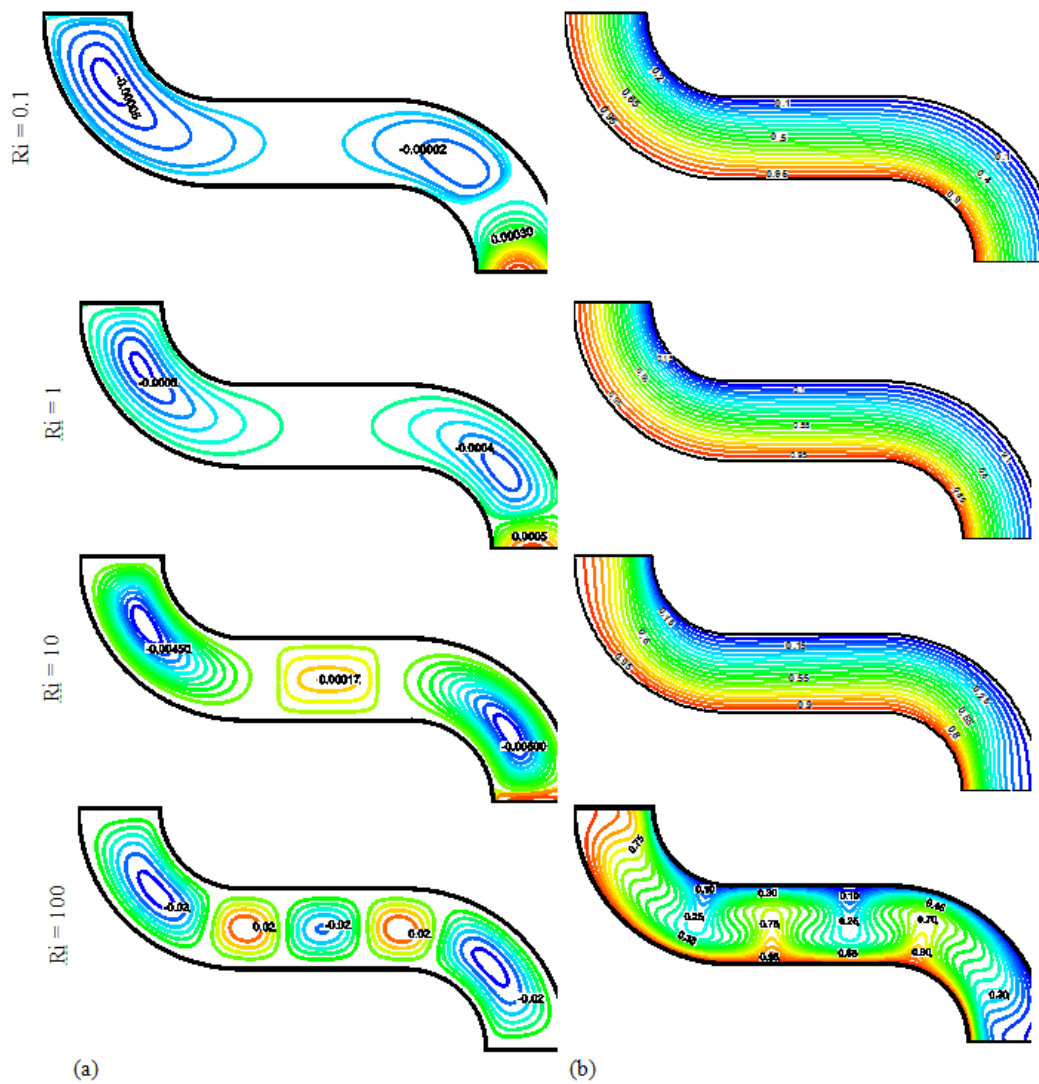


Figure 4 (a) Streamline and (b) isotherm plots for different values of Ri while $Pr=6.2$, $Ha=10$, $\phi = 1\%$ and $Re = 50$.

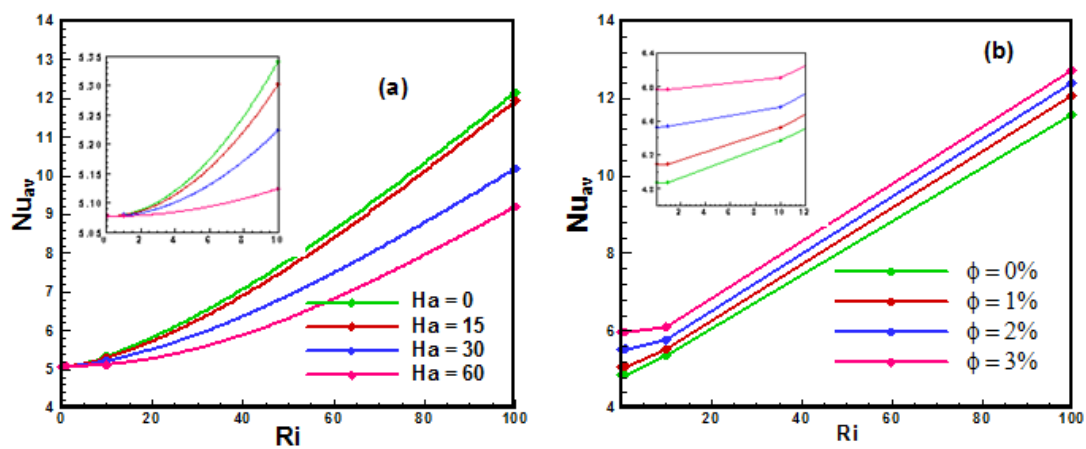


Figure 5 Variation of average Nusselt number against Ri with different Ha and ϕ at $Pr = 6.2$, and $Re = 50$.

Conclusion

In this study, mixed convection flow in a nanofluid field tubular enclosure was numerically investigated. The finite element method is used to solve the governing equations. A detailed parametric analysis has been done and discussed elaborately from the physical point of view. Numerical and graphical validation tests have been performed and found it in good agreements. Based on the graphical presentation and discussion, the findings of this study can be summarized as follows:

- a. Fluid motion increases significantly with increasing of Richardson number.
- b. Temperature distribution depends on the Richardson number.
- c. The increase in Richardson number increases the natural convection mode as well as heat transfer rate.
- d. The increase in heat transfer rate accelerates with the addition of nanoparticles and decelerates with increasing of Hartmann number.
- e. Heat transfer rate is important in nanofluid compared to base fluid.

As the present study has been numerically accomplished, experimental work is required for the better understanding of the numerical findings.

Acknowledgments

None.

Conflicts of interest

The authors declare that are no conflicts of interest.

References

1. Rahman MM, Alim MA, Saha S, et al. Effect of the presence of a heat conducting horizontal square block on mixed convection inside a vented square cavity. *Nonlinear Analysis: Modelling and Control*. 2009;14(4):531–548.
2. Basak T, Roy S, Singh SK, et al. Analysis of mixed convection in a lid-driven porous square cavity with linearly heated side wall (s). *International journal of heat and mass transfer*. 2010;53(9-10):1819–1840.
3. Ismael MA, Pop I, Chamkha AJ, et al. Mixed convection in a lid-driven square cavity with partial slip. *International Journal of Thermal Sciences*. 2014;(82):47–61.
4. Mittal N, Satheesh A, Santhosh Kumar D, et al. Numerical simulation of mixed convection flow in a lid driven porous cavity using different nanofluids. *Heat Transfer/Asian Research*. 2014;43(1):1–16.
5. Ali MM, Alim MA, Ahmed SS, et al. Magneto hydrodynamic mixed convection flow in a hexagonal enclosure. *Procedia engineering*. 2017;(194):479–486.
6. Ali MM, Alim MA, Ahmed SS et al. Oriented magnetic field effect on mixed convective flow of nanofluid in a grooved channel with internal rotating cylindrical heat source. *International Journal of Mechanical Sciences*. 2019;(151):385–409.
7. Rashidi MM, Nasiri M, Khezerloo M, et al. Numerical investigation of magnetic field effect on mixed convection heat transfer of nanofluid in a channel with sinusoidal walls. *Journal of Magnetism and Magnetic Materials*. 2016;(401):159–168.
8. Kareem AK, Mohammed HA, Hussein AK, et al. Numerical investigation of mixed convection heat transfer of nanofluids in a lid-driven trapezoidal cavity. *International Communications in Heat and Mass Transfer*. 2016;(77):195–205.
9. Javed T, Mehmood Z, Pop I, et al. MHD-mixed convection flow in a lid-driven trapezoidal cavity under uniformly/non-uniformly heated bottom wall. *International Journal of Numerical Methods for Heat & Fluid Flow*. 2017;27(6):1231–1248.
10. Abbaszadeh M, Ababaei A, Arani AAA, et al. MHD forced convection and entropy generation of CuO-water nanofluid in a microchannel considering slip velocity and temperature jump. *Journal of the Brazilian Society of Mechanical Sciences and Engineering*. 2017;(39):775–790.
11. Nasrin R, Alim MA, Chamkha AJ, et al. Buoyancy-driven heat transfer of water–Al₂O₃ nanofluid in a closed chamber: effects of solid volume fraction, Prandtl number and aspect ratio. *International Communications in Heat and Mass Transfer*. 2012;(55):7355–7365.
12. Taylor C, Hood P. A numerical solution of the Navier-Stokes equations using the finite element technique. *Computers & Fluids*. 1973;1(1):73–100.
13. Dechaumphai P. *Finite Element Method in Engineering*. 2nd ed. Bangkok: Chulalongkorn University Press; 1999.
14. Basak T, Roy S, Sharma PK, et al. Analysis of mixed convection flows within a square cavity with uniform and non-uniform heating of bottom wall. *International Journal of Thermal Sciences*. 2009;48(5):891–912.
15. Rahman MM, Alim MA. MHD mixed convection flow in a vertical lid-driven square enclosure including a heat conducting horizontal circular cylinder with Joule heating. *Nonlinear Analysis: Modelling and Control*. 2010;15(2):99–211.